IOPscience iopscience.iop.org

Home Search Collections Journals About Contact us My IOPscience

Local structures and relative stabilities of Tl^{+}-dimer substitutional impurity centres in NaI and KI

This article has been downloaded from IOPscience. Please scroll down to see the full text article.

2001 J. Phys.: Condens. Matter 13 8015

(http://iopscience.iop.org/0953-8984/13/35/309)

View the table of contents for this issue, or go to the journal homepage for more

Download details:
IP Address: 171.66.16.226
The article was downloaded on 16/05/2010 at 14:48

Please note that terms and conditions apply.

INSTITUTE OF PHYSICS PUBLISHING JOURNAL OF PHYSICS: CONDENSED MATTER

J. Phys.: Condens. Matter **13** (2001) 8015–8029 PII: S0953-8984(01)24826-7

Local structures and relative stabilities of Tl^+-dimer substitutional impurity centres in NaI and KI

Andrés Aguado

Physical and Theoretical Chemistry Laboratory, University of Oxford, South Parks Road, Oxford OX1 3QZ, UK

Received 15 May 2001, in final form 3 July 2001
Published 16 August 2001
Online at stacks.iop.org/JPhysCM/13/8015

Abstract

The local lattice distortions around a Tl^+-dimer substitutional impurity in NaI and KI have been investigated by using a mixed *ab initio*/parametrized methodology. One important conclusion of the work is that an explicit consideration of these distortions up to at least the first four coordination shells of ions around the impurity is needed in order to achieve a converged result for the first- and second-shell distortions. After describing the lattice distortions induced by both D_{4h} and D_{2h} configurations, we analyse their relative stability by calculating the defect formation energies. It is found that the D_{4h} configuration is lower in energy for both crystals, but the energy difference is so small in the case of the NaI host lattice that the two configurations can be considered degenerate for all practical purposes. It is also found that inclusion of polarization interactions is crucial in the stabilization of the defect in NaI.

1. Introduction

The local distortions induced by substitutional impurities in ionic crystals are important quantities as they determine the crystal field exerted on the impurity by the host lattice, and thus the specific absorption/emission properties of the system [1]. While the optical properties of these doped crystals are directly accessible to experiment, the structural lattice distortions are much more difficult to determine [2–4]. Thus, reliable theoretical calculations are an ideal complement to experimental studies in this field [5].

When the impurity concentration is low, the interaction between different substitutional impurities can be neglected, and the lattice distortion induced by a single isolated impurity is all that needs to be considered. The most important factor affecting the lattice distortions in that case is the charge state of the impurity:

(a) If the substitutional impurity ion is isovalent with one of the lattice ions, the distortions are mainly determined by the mismatch (packing) effect arising from the different sizes of the ions involved [6–8].

 © 2001 IOP Publishing Ltd Printed in the UK

(b) If the substitutional impurity carries a formal charge different from that of the substituted lattice ion, then Coulomb electrostatic effects are more important. Moreover, charge compensation usually requires the creation of nearby lattice defects around the impurity, which complicates the analysis of the structural distortions quite a bit [9, 10].

With increasing concentration of the dopant, the interaction between impurities centred on different lattice sites can no longer be neglected, and eventually aggregation of impurity centres occurs, leading to the formation of dimer centres, trimer centres etc. The dimer centres of impurity ions with the ns^2 outer electronic configuration have been considered in detail by Tsuboi and Jacobs [11]. They lead to new, specific absorption/emission lines that can be difficult to resolve experimentally due to the considerable overlap with the lines arising from the isolated impurity centres, whose concentration is always higher. Nevertheless, experimental reports on the optical properties of these dimer centres in different alkali halide host lattices have been published throughout the years [12–26]. More complicated aggregate centres involving ns^2 substitutional ions have also been observed [27–30]. Knowledge of just the absorption/emission properties does not permit one to make definite statements about the geometric structure of the defect complex, however. Two different configurations are possible in principle: (a) the D_{2h} configuration, in which the two impurity ions are nearest-neighbour cations along the (110) crystallographic axes; (b) the D_{4h} configuration, where those two impurity ions are next-nearest-neighbour cations lying along the (100) crystallographic axes. There has been a long and controversial debate regarding which configuration is energetically more stable. Experimentally, some insight into this problem can be gained by measuring the azimuthal polarization dependence of the luminescence. In this way, some authors [31–33] have claimed to have found enough evidence to support a D_{4h} ground-state configuration of the dimer centres in NaI, KCl and KI, while some others [16, 34–37] have interpreted their experiments in terms of a D_{2h} defect configuration in KBr, KI and RbI. Tsuboi has pointed out that his latest results [26, 35, 36] do not exclude the possibility of D_{4h} defect centres. The point is that the specific luminescence of D_{4h} centres is hard to observe because, since the Tl^+ cations are less perturbed compared to the D_{2h} configuration, the optical lines overlap to a larger extent with those arising from the isolated impurity centres, and so are more difficult to resolve. In summary, the feeling is that the situation is far from being clear at the moment. From the theoretical side, the author is aware of just one, very recent, article, by Pascual, Barandiarán and Seijo [38], dealing with the lattice distortions induced by both Tl-monomer and Tl-dimer centres in KCl. Thus, there is still a strong need for first-principles calculations to help in disentangling this interesting structural problem. This will be the main goal of the present contribution.

With these ideas in mind, we have employed the *ab initio* perturbed-ion (aiPI) model [39–44] to study the lattice distortions induced by a substitutional Tl^+ dimer in NaI and KI. The model has been enlarged by inclusion of a parametrized potential model accounting for the effects of dispersion and polarization interactions. The mixed *ab initio*/semiempirical model thus obtained is a very convenient and powerful tool for modelling impurity systems, as it has the following desirable properties:

(a) The local region around the impurity can be modelled by a large active cluster embedded in a quantum-mechanical description of the surrounding crystalline lattice [45].
(b) The computational cost of the model increases just linearly with the number of symmetry-inequivalent ions included in the active cluster [46], allowing for the structural relaxation of several coordination shells of ions with a reasonable effort.
(c) The connection between the local region around the defect in which structural rearrangements are important and the frozen crystalline environment is made through a smooth

interface formed by fixed ions whose wavefunctions are allowed to self-consistently relax [47, 48].

(d) The systematic errors of the model are estimated by performing parallel cluster calculations on the pure crystals [47, 48].

The remainder of this paper is organized as follows. In section 2 we describe the active clusters which have been used to model the doped systems, together with a description of the energy model employed. In section 3 we present and discuss the results of the calculations and section 4 summarizes the main conclusions.

2. Cluster model

The aiPI model is a particular application of the Hartree–Fock version of the theory of electronic separability of Huzinaga and co-workers [49, 50] to ionic solids, in which the basic building blocks are reduced to single ions, and was first developed for the study of perfect crystals [39]. In brief, the crystal wavefunction is assumed to be an antisymmetrized product of monocentre ionic wavefunctions. The dispersion interactions, coming from the interionic electron Coulomb correlation, are neglected in this approximation and will have to be reintroduced later on. The variational principle applied to the Hamiltonian operator, together with the restriction (introduced by means of a Lagrange multiplier) that the ionic wavefunctions obey strong orthogonality conditions [51], leads to the following set of Fock-like equations, one for each active ion R in the crystal:

$$H_{eff}^{R}|\psi^{R}\rangle = E_{eff}^{R}|\psi^{R}\rangle \tag{1}$$

where the effective Hamiltonian is a sum of one-electron and two-electron contributions:

$$H_{eff}^{R} = \sum_{i=1}^{N_R} h_{eff}^{R}(i) + \sum_{1\leqslant j<i\leqslant N_R} r_{ij}^{-1} \tag{2}$$

with

$$h_{eff}^{R}(i) = T(i) - Z^{R} r_{iR}^{-1} + \sum_{S\neq R}[V_{env}^{S}(i) + P^{S}(i)] \tag{3}$$

$$V_{env}^{S}(i) = -Z^{S} r_{is}^{-1} + V_{C}^{S}(i) + V_{X}^{S}(i). \tag{4}$$

Thus, the effective Hamiltonian for ion R contains, apart from the usual intra-atomic terms (electronic kinetic energy, attraction of the electrons of ion R to the nucleus of ion R and Coulomb, exchange and correlation interactions between electrons of ion R), an additional environmental potential taking account of both classical (Coulomb) and quantum (exchange and orthogonality) interactions between the electrons of ion R and the electrons and nuclei of the (frozen) environment. The electronic Coulomb interaction term $V_C^S(i)$ is usefully decomposed into two terms, one accounting for the Madelung interaction between point-like formal charges and the other accounting for the correction to that Madelung term arising from the finite extent of the ionic electron densities (this term has been called a *penetration* term by Pyper) [52]. Finally, it has been shown that the expectation value of the lattice projection operator $P^S(i)$ (the operator that enforces the strong-orthogonality conditions on the orbitals centred in two different ions) can be identified with the overlap repulsive energy [53]. $P^S(i)$ and $V_X^S(i)$ are the only operators that involve an interchange of electronic labels between electrons on two different ions, and therefore their sum can be identified with the *permutation* term introduced by Pyper [52]. This completes the description of the electronic interactions, to which the nuclear–nuclear term is added in order to obtain the total effective energy E_{eff}^R. The aiPI calculations

for a perfect crystal consist in the iterative resolution of equation (1) in the frozen environment provided by the solutions of the previous cycle, in such a way that full ion–lattice consistency is achieved at the end of the process. When that self-consistent process is finished [54], the outputs are a set of consistent crystal wavefunctions, one for each inequivalent ion in the lattice, and the effective energies of each of the ions. These effective energies can be usefully decomposed into two terms:

$$E^R_{eff} = E^R_{re} + E^R_{int} \tag{5}$$

where the interaction energy term contains all the pairwise interactions (Madelung, penetration and permutation) and the rearrangement term accounts for the many-body energy contribution associated with the compression of the ion by the environment (it is a repulsive contribution on account of the kinetic energy increase experienced by the electronic cloud), and incorporates the intraionic electron correlation, estimated by employing the Coulomb–Hartree–Fock model [55–57]. The model could be useful in the parametrization of the so-called compressible-ion models (CIM) [58–60], with a very modest computational effort. To obtain the total energy of the crystal, one just has to avoid double counting of the interaction energies:

$$E_{crystal} = \sum_R (E^R_{re} + (1/2)E^R_{int}). \tag{6}$$

The application of the aiPI model to the study of impurity centres in ionic crystals makes use of the cluster approach, and has been fully described in references [46–48]. The basic assumption of a cluster approach is that all the relevant physico-chemical changes induced by the introduction of a substitutional impurity into the host lattice are short ranged and therefore localized in a finite region around the impurity. Correspondingly, the doped crystal is divided into two regions, which we call **C** (the cluster) and **L** (the lattice). The **C** region contains the impurity and those lattice ions around it that are supposed to be directly affected by the presence of the impurity. The **L** region is formed by all those lattice ions outside the **C** region. When using the cluster approach, one has to provide accurate enough descriptions for both regions, as well as for the interactions between those regions. Within the aiPI methodology, this is achieved in the following way: the region **L** is further divided into two regions $\mathbf{L}^{\text{near}}$ and $\mathbf{L}^{\text{far}}$. The ions in the region $\mathbf{L}^{\text{near}}$ are represented by frozen wavefunctions extracted from a reference aiPI calculation performed on the corresponding pure crystal. These ions act on the ionic electron densities of the ions in region **C** through both classical and quantal lattice interactions, as described in the previous paragraph. The $\mathbf{L}^{\text{near}}$ region extends up to a distance such that the quantal contributions to the effective energy of region **C** are negligibly small (in practice less than 10^{-6} Hartree). Lattice ions located at longer distances act on region **C** just through the point-like Madelung interaction. Thus, the ions in this region $\mathbf{L}^{\text{far}}$ are represented by simple point charges, until a good representation of the Madelung potential inside the **C** region is achieved. Within the **C** region, called the active cluster, the aiPI equations as described above are explicitly solved, including the effect of the frozen environmental potential provided by the **L** region. Thus, at the end of the self-consistent procedure, an ion–ion consistency is achieved within the active cluster, and at the same time each ionic wavefunction in set **C** is consistent with the frozen description of the surrounding lattice. To calculate the lattice distortions, the active cluster is also divided into two smaller subsets, which we call $\mathbf{C}_1$ and $\mathbf{C}_2$. Both the wavefunctions and the positions of all ions within region $\mathbf{C}_1$ are allowed to relax. In contrast, only the wavefunctions of the ions in region $\mathbf{C}_2$ are allowed to self-consistently adapt to the changing potential. In practice, region $\mathbf{C}_2$ is formed by all those ions that are nearest neighbours of the ions in region $\mathbf{C}_1$ and are not already included in $\mathbf{C}_1$. Thus, region $\mathbf{C}_2$ provides a smooth interface of fixed but electronically deformable ions linking the $\mathbf{C}_1$ region, where distortions are important, with the frozen lattice, and its introduction has been

shown to be necessary in order to obtain acceptable distortions [6–10]. The only region that still has to be described is thus $\mathbf{C}_1$. In this work, we have chosen to include within $\mathbf{C}_1$ the two Tl^+ impurity cations, plus their first four coordination shells, plus their seventh coordination shell. These clusters contain 58 and 61 ions for the D_{2h} and D_{4h} defects, respectively. The corresponding number of ions within the total active clusters ($\mathbf{C}_1$ plus $\mathbf{C}_2$ subsets) are 160 and 163. On the technical side, we have used large STO basis sets for the description of the ions, all taken from Clementi–Roetti [61] and McLean–McLean [62] tables. All calculations have been performed by employing the experimental lattice constants [63] to describe the geometrically frozen part of the crystals.

In the present version of the aiPI code, the ion–electron densities are forced to remain spherically symmetric, which is correct for the high-symmetry environment experienced by the ions in the pure crystals but not for the distorted configurations found in the doped crystals. Thus, we have enlarged our energy model by inclusion of a parametrized potential model description of polarization interactions. Specifically, we have employed the polarizable-ion model (PIM) devised by Madden and co-workers [64,65], as explained in previous publications [66, 67]. This is a model that allows for a proper representation of both asymptotic and short-range effects on the polarizabilities. Its parametrization has been performed by employing as input the results of highly accurate *ab initio* calculations, as opposed to experimental input. Moreover, careful parametrization strategies were employed to ensure that no mixing of different physical effects occurs in each separate parameter, improving thus on the results of shell-model calculations. This is reflected in the fact that parameters for closely related materials can be deduced from those for a reference system by simple scaling arguments involving ion radii [65, 68]. As the in-crystal anion polarizabilities were obtained from experimental crystal values, following reference [69], the procedure should be highly reliable. The short-range parameters appropriate to our systems were obtained through the scaling procedures validated in references [65, 68].

As we have already stated, dispersion interactions are also absent from the present methodology. These can be included in our energy model by following the methods described by Pyper [70, 71]. Specifically, the dipole–dipole C_6-coefficient is obtained from the ionic polarizabilities through the Slater–Kirkwood formula [72]. This has been shown by Pyper [70] to be the most reliable method for obtaining such coefficients.

Now we discuss the method employed to obtain the lattice distortions. The total number of structural parameters involved in the optimization of the effective energy of the active cluster is quite large (specifically, 17 for the D_{4h} defect and 31 for the D_{2h} defect—see the next section). These numbers are imposed by forcing the active cluster to have the exact symmetry of those two group points, as a consideration of a larger number of parameters would be computationally troublesome. Searching for the global energy minimum in hyperspaces of such high dimensionalities is far from trivial, and a direct search would be computationally very expensive. We have thus adopted a stepped procedure, which consists of iteratively relaxing each coordination shell. In a first step, only the positions of those ions in the first coordination shell are allowed to vary. Then those ions are fixed at their optimal positions and optimization of the second coordination shell proceeds. When the seventh coordination shell has been relaxed, the procedure starts again with the relaxing of the first one. This relaxation process is stopped when the values of all 17 (31) parameters in a new cycle are the same as those of the previous cycle, up to a given tolerance. It has been found that only four external cycles are needed in order to obtain converged distortions. To acquire reasonable confidence that we have really found the global minimum, we have given several random displacements to the ions (starting from the optimized configuration) and checked that the ions always come back to the same minimum. An interesting aspect of this stepped procedure is that one can

analyse the importance of the inclusion of the geometrical relaxation of additional shells in obtaining a converged value for the distortion of the first shell, which is the only one included in the vast majority of *ab initio* calculations on doped crystals. The specific values of the distortions have been calculated taking account of the nonperfect self-embedding consistency of the model [6–10]:

$$\Delta U_i = U_i((\mathrm{Tl}^+)_2{:}\mathrm{AX}) - U_i(\mathrm{A}^+{:}\mathrm{AX}) \tag{7}$$

where $U_i((\mathrm{Tl}^+)_2{:}\mathrm{AX})$ are the equilibrium values adopted by the structural parameters employed to characterize the geometry of the active cluster (see the next section) in the doped crystal, and $U_i(\mathrm{A}^+{:}\mathrm{AX})$ are the equilibrium values adopted by those same parameters when describing the pure crystal with the same cluster model as was employed to describe the doped crystal. Thus, any inaccuracy related to a wrong description of the pure crystal (always very small in practice) is cancelled out in the difference.

We finish this section with a brief discussion of the expected reliability of the distortions obtained. We are employing a mixed *ab initio*/parametrized model, which implies that our representation of the several interactions cannot be as accurate as that obtained from purely *ab initio* models. The most important short-range quantal terms are, however, calculated with an *ab initio* code. The only parametrized terms (polarization and dispersion) were obtained by employing parameters extracted from highly reliable *ab initio* calculations, and introducing those parameters into well tested models for those two interactions. Thus, our opinion is that the representation of these two terms is highly accurate. Nevertheless, there still remain three possible sources of error:

(a) The calculations are not relativistic. Although relativistic effects are known to have an important influence on the optical spectra, we do not expect them to have a marked effect on the lattice distortions.
(b) Although we have introduced the electrostatic polarization energy through the PIM model, the ionic electron densities continue to be spherical. In distorted environments, these ionic electron densities are expected to assume aspherical shapes, which can have an effect on the short-range repulsive overlap energies. An aspherical ion model (AIM) accounting for such effects has also been introduced by Rowley *et al* [59]. These authors find that AIM effects are only important for the description of some dynamical properties of ionic metal oxides, while their effect on the static properties of alkali halides is expected to be negligibly small.
(c) Were the effects described in (a) and (b) be included in our model, we would be working with a complete ionic description of the system. Covalent interactions, associated with charge transfer between the ions, would continue to be neglected. It is the author's view, however, that an ionic description (that is, with any charge transfer neglected) of the systems under consideration should be essentially correct.

To support these expectations, we offer a comparison between the results obtained previously by the author on the first-shell distortion around a Tl-monomer centre in NaI, NaCl and KCl [8], and those obtained by other authors employing more involved electronic structure calculations [38, 73, 74]. Pascual *et al* [38] obtained an expansion of between 2% and 3% for KCl:Tl^+ (depending on the introduction or neglect of lattice relaxation and polarization effects), which is essentially the same as that obtained by the author in reference [8]. Similarly, the expansion of 8% obtained for NaCl:Tl^+ in reference [73] compares very well with that obtained in reference [8], namely about 6%. Finally, the 5% expansion found by Barriuso *et al* [74] in NaI:Tl^+ compares equally well with the aiPI value of about 6%. This last value is given here for the first time; it was obtained employing exactly the same cluster model as that described

in reference [8]. The quantitative value given in reference [6] for that expansion, namely 1%, was wrong due to an inaccurate representation of the projection operator enforcing the ion–lattice orthogonality [75], which was corrected in all subsequent publications. The main qualitative result of reference [6], namely that the lattice distortion induced by the impurity affects several coordination shells around it, continues to be valid in our opinion, however. In summary, we believe we have shown that our results can compete in accuracy with those obtained from more involved electronic structure calculations—even more so if we realize that we can take advantage of the good scaling properties obtained after simplifying the energy model and consider large active clusters, with an explicit consideration of the relaxation of several coordination shells.

An alternative accuracy check is provided by a consideration of the pure crystals NaI, KI and TlI. If the method is able to provide accurate values for the interionic distances of these three crystals, then we expect the description of the impurity systems to be similarly accurate. The aiPI equilibrium distances for the rock-salt phase of the alkali halide crystals are $d(\mathrm{NaI}) = 3.236$ Å and $d(\mathrm{KI}) = 3.533$ Å, in very good agreement with the experimental results [63]. Thus, fixing the interionic distances of the frozen environment to the experimental distances (see above) is a good approximation. TlI crystallizes at low temperature in an orthorhombic $Cmcm$ structure, with cell parameters $a = 4.582$ Å, $b = 12.92$ Å and $c = 5.251$ Å. The ion positions within the unit cell are given by $(0, u, 1/4)$, $(0, -u, 3/4)$, $(1/2, u+1/2, 1/4)$ and $(1/2, 1/2-u, 3/4)$, with $u(\mathrm{I}) = 0.1333$ and $u(\mathrm{Tl}) = 0.392$ [76]. The results from our hybrid method are $a = 4.603$ Å, $b = 12.98$ Å, $c = 5.286$ Å, $u(\mathrm{I}) = 0.1318$ and $u(\mathrm{Tl}) = 0.3931$. The agreement is seen to be very good, which shows that the covalent effects are not very important even for this low-gap material. The cell volume obtained is slightly larger than the experimental one. We ascribe this to our neglect of relativistic effects, which are known to induce a slight contraction of interionic distances in compounds of this type [77–80]. This alternative test confirms the conclusions in the previous paragraph and gives support to the credibility of our results.

3. Results and discussion

3.1. D_{4h} and D_{2h} distortions

The results for the lattice distortions induced by the D_{4h} centre are shown quantitatively in table 1 (we do not show explicitly the seventh-shell distortions because these are always very small). For the first and second coordination shells, they are also shown schematically in figure 1. Note that, due to the symmetry of the defect, the origin has been placed in the iodide anion bridging the two Tl^+ impurities. During the optimization process, this anion is fixed at the $(0, 0, 0)$ lattice site without loss of generality. In general, we can see that the first shell of anions expands as a result of the introduction of the $(Tl^+)_2$ dimer, by an amount which is larger in NaI as compared to KI. This is the expected behaviour, as the mismatch ion size effect is more acute in NaI than in KI. There are additional differences between the two systems: in NaI, the Tl^+–I^- distances along the (001) direction are approximately the same, and smaller than the Tl^+–I^- equilibrium distances along (100) and (010) directions; for KI, in contrast, ΔU_2 is approximately equal to ΔU_1, and so the two iodide ions located at $(0, 0, 1)$ crystallographic sites do not experience any expansion at all, while the expansions experienced by all other first-shell anions are approximately the same. In both crystals, the eight iodide anions located at $(1/2, 0, 1/2)$ and equivalent lattice sites also experience small negative out-of-plane distortions, that help to further reduce the Tl^+–I^- overlap repulsion. These first-shell distortions are strongly coupled to the distortions experienced by the other coordination shells,

Table 1. Lattice distortions (in Å) of several coordination shells around the D_{4h} Tl^+-dimer defect in NaI and KI. The quantities ΔR_i, where they appear, are defined as $\Delta R_i = \sqrt{2}\Delta U_i$; that is, they measure polar distances. The optimization parameters, U_i, together with their pure crystal values in crystallographic units, are shown explicitly, as well as the number of symmetry-equivalent ions in each coordination shell.

Coordination shell	Ionic site	Degeneracy	Pure crystal value	Distortion	NaI	KI
First	$(0, 0, U_1)$	2	$U_1 = 1/2$	ΔU_1	0.109	0.049
	$(0, 0, U_2)$	2	$U_2 = 1$	ΔU_2	0.208	0.046
	$(U_3, 0, U_4)$	8	$U_3 = 1/2$	ΔU_3	0.168	0.043
			$U_4 = 1/2$	ΔU_4	−0.021	−0.025
Second	$(U_1, 0, 0)$	4	$U_1 = 1/2$	ΔU_1	0.135	0.077
	$(U_2, 0, U_3)$	8	$U_2 = 1/2$	ΔU_2	0.099	0.072
			$U_3 = 1$	ΔU_3	0.122	0.092
	(U_4, U_4, U_5)	8	$U_4 = 1/2$	ΔR_4	0.134	0.109
			$U_5 = 1/2$	ΔU_4	0.015	−0.001
Third	(U_1, U_1, U_2)	8	$U_1 = 1/2$	ΔR_1	−0.084	−0.096
			$U_2 = 1$	ΔU_2	−0.064	−0.084
	$(U_3, U_3, 0)$	4	$U_3 = 1/2$	ΔR_3	−0.097	−0.098
Fourth	$(0, 0, U_1)$	2	$U_1 = 3/2$	ΔU_1	0.082	0.072
	$(U_2, 0, U_3)$	8	$U_2 = 1$	ΔU_2	0.086	0.070
			$U_3 = 1/2$	ΔU_3	0.034	0.038

as we have discussed in detail in a previous publication [8]. As an example, if we just allow for the displacement of the first coordination shell of ions (corresponding to the first step of our optimization procedure—see the previous section), the ΔU_i distortions (in Å) in KI:$(Tl^+)_2$ are found to be 0.010, −0.015, −0.013 and −0.030 for $i = 1, 2, 3$ and 4, respectively. These values are very different from the converged ones shown in table 1. Sometimes even the sign of the distortion is erroneously predicted. A consideration of lattice relaxation effects of a larger number of coordination shells is thus mandatory for these systems.

The size mismatch effect also increases the short-range repulsions from the lattice cations in the second coordination shell, which expands in response to this. Again this expansion is larger in NaI as compared to KI. For those cations located at $(1/2, 0, 1)$ and equivalent sites, the expansion is larger along the z-axis. We can easily understand that this is due to a coupling with the first-shell distortion. Specifically, the expansion of the first-shell anions at $(1/2, 0, 1/2)$ and equivalent sites reduces the screening of the Coulomb repulsion with the cations located at $(1/2, 0, 0)$ and equivalent sites (see figure 1). To confirm this expectation, one can perform a hypothetical calculation of the distortion including only the second shell and not the first-, third- and fourth-shell displacements. When this is done, the difference between ΔU_2 and ΔU_3 is almost negligible. The anions forming the third coordination shell experience a contraction, which is the same result as was obtained in reference [8] for the Tl^+-monomer centre in alkali halides. The distortion of this shell is almost isotropic, so it is not too much affected by the reduction of symmetry. Finally, the fourth coordination shell, formed by cations, experiences an appreciable expansion according to our model, but considerably smaller than the first-shell expansion, as expected. In order to obtain a converged value for the fourth-shell distortions, the inclusion of seventh-shell distortions was mandatory. Specifically, a much larger (approximately twice as large) fourth-shell expansion is predicted when fixing the positions of the ions in the seventh coordination shell to their pure crystal values. This is analogous to the first-shell situation discussed in the previous paragraph.

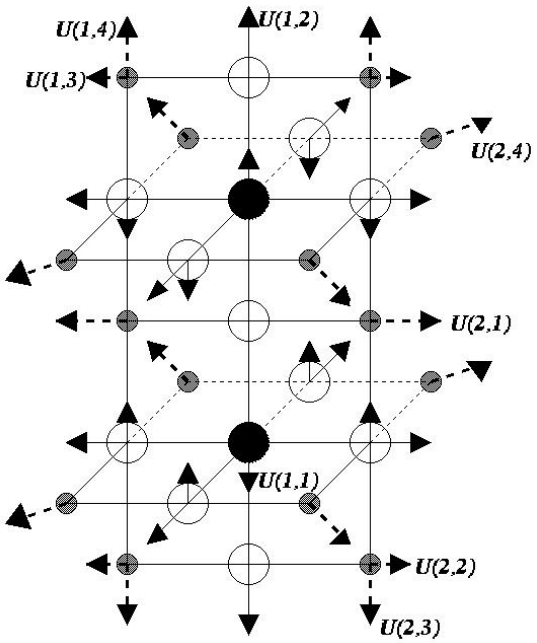

Figure 1. A qualitative illustration of the first- and second-shell distortions around the D_{4h} Tl^+-dimer defect in NaI. Large filled balls are Tl^+ cations, large empty balls are I^- anions and small shaded balls are Na^+ cations. To help with the visualization, not all second-shell cations are explicitly shown. The notation $U(m, n)$ specifies the distortion ΔU_n experienced by the ions in the mth coordination shell (see table 1 for quantitative values).

The lattice distortions induced by the D_{2h} dimer centre are shown in table 2 and figure 2, in an analogous way to that employed for the D_{4h} centre. Due to the symmetry properties, we have located the origin of the active cluster at the $(1/4, 1/4, 0)$ crystallographic position in this case. Now the two Tl^+ impurities are nearest-neighbour cations along the (110) crystallographic axes, and their direct overlap interactions become important. As a result of these, an increase of the Tl^+–Tl^+ distance by roughly 0.06 Å with respect to the pure host lattice value is observed, which is quite independent of the specific pure crystal. This means that the equilibrium Tl^+–Tl^+ distance in NaI is smaller than that found in KI by a factor of $\approx a(\mathrm{NaI})/a(\mathrm{KI})$, with a the lattice constant of the respective crystal. The two first-shell anions at $(U_2, -U_2, 0)$ sites expand appreciably along the $(1\bar{1}0)$ crystallographic axes in NaI, but the corresponding expansion is almost negligible in KI. The other eight first-shell anions similarly experience expansions which are always larger in the case of NaI. Note that, for both crystals, the expansion is largest for the anions at $(U_3, U_4, 0)$ and smallest for those located at $(U_2, -U_2, 0)$, this trend correlating with the expansion of the two impurity cations. Also, a significant expansion along the (110) axes of the anions located at (U_5, U_5, U_6) is observed in NaI. This displacement helps to keep those anions almost on top of the Tl^+ cations along the (001) directions. This is not observed in the case of KI. By way of a reference, we quote here again the values obtained for the first-shell displacements ΔU_i around the D_{2h} defect in KI when only that shell is allowed to relax. They are (in Å) -0.010, 0.004, -0.019, 0.01, 0.039 and -0.018 for $i = 1$, 2, 3, 4, 5 and 6, respectively. As we can see, a contraction of the Tl^+–Tl^+ distance (with respect to the pure crystal value) is predicted, together with corresponding contractions of some of the first-shell iodides. Similarly to the D_{4h} case, we find that relaxation of a larger number of shells

Table 2. Lattice distortions (in Å) of several coordination shells around the D_{2h} Tl^+-dimer defect in NaI and KI. The quantities ΔR_i, where they appear, are defined as $\Delta R_i = \sqrt{2}\Delta U_i$; that is, they measure polar distances. The optimization parameters, U_i, together with their pure crystal values in crystallographic units, are shown explicitly, as well as the number of symmetry-equivalent ions in each coordination shell.

Coordination shell	Ionic site	Degeneracy	Pure crystal value	Distortion	NaI	KI
First	$(U_1, U_1, 0)$	2	$U_1 = 1/4$	ΔR_1	0.055	0.057
	$(U_2, -U_2, 0)$	2	$U_2 = 1/4$	ΔR_2	0.203	0.009
	$(U_3, U_4, 0)$	4	$U_3 = 3/4$	ΔU_3	0.186	0.043
			$U_4 = 1/4$	ΔU_4	−0.010	−0.016
	(U_5, U_5, U_6)	4	$U_5 = 3/4$	ΔR_5	0.047	0.008
			$U_6 = 1/2$	ΔU_6	0.154	0.032
Second	$(U_1, U_1, 0)$	2	$U_1 = 3/4$	ΔR_1	0.150	0.117
	$(U_2, -U_3, 0)$	4	$U_2 = 1/4$	ΔU_2	0.075	0.062
			$U_3 = 3/4$	ΔU_3	0.146	0.102
	$(U_4, -U_4, U_5)$	4	$U_4 = 1/4$	ΔR_4	0.061	−0.007
			$U_5 = 1/2$	ΔU_5	0.142	0.075
	(U_6, U_7, U_8)	8	$U_6 = 3/4$	ΔU_6	0.119	0.093
			$U_7 = 1/4$	ΔU_7	0.004	—
			$U_8 = 1/2$	ΔU_8	0.092	0.073
Third	(U_1, U_1, U_2)	4	$U_1 = 3/4$	ΔR_1	−0.095	−0.112
			$U_2 = 1/2$	ΔU_2	−0.059	−0.071
	$(U_3, -U_4, U_5)$	8	$U_3 = 1/4$	ΔU_3	−0.047	−0.055
			$U_4 = 3/4$	ΔU_4	−0.048	−0.084
			$U_5 = 1/2$	ΔU_5	−0.044	−0.066
Fourth	$(U_1, U_2, 0)$	4	$U_1 = 5/4$	ΔU_1	0.083	0.069
			$U_2 = 1/4$	ΔU_2	0.012	0.007
	(U_3, U_3, U_4)	4	$U_3 = 1/4$	ΔR_3	−0.031	−0.033
			$U_4 = 1$	ΔU_4	0.077	0.064

is an important ingredient in obtaining converged first-shell distortions. In general, the second, third and fourth coordination shells relax following the same patterns as were described for the D_{4h} case.

Next we would like to analyse here the convergence of our distortions. As we have already stated, the distortions in each shell are strongly coupled to those of other shells. The strongest and therefore most important coupling is found to be that between first and second shells. Thus, our opinion is that at least those two shells should be included in cluster calculations of defects. We have explicitly checked, by including relaxation of a larger number of ions along (110) crystallographic directions, that the distortions presented for the second shell are well converged. We have not found, either, substantial modifications in the third-shell distortions when including more ions along (111) directions. Another important coupling is that between distortions along (100) directions: it is necessary to include fourth-shell distortions in order to obtain converged first-shell distortions; similarly, it is necessary to include seventh-shell distortions in order to obtain converged fourth-shell distortions. As the seventh-shell distortions are themselves quite small (below 0.02 Å), we think that the distortions along (100) directions do not propagate beyond that shell.

To the best of the author's knowledge, there is only one other first-principles electronic structure calculation dealing with the distortions induced by a Tl^+-dimer centre, in that case in

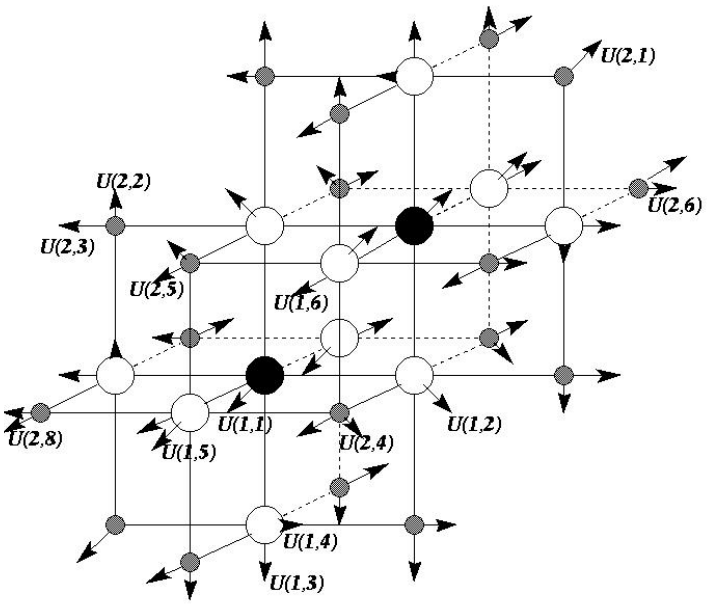

Figure 2. A qualitative illustration of the first- and second-shell distortions around the D_{2h} Tl^+-dimer defect in NaI. Large filled balls are Tl^+ cations, large empty balls are I^- anions and small shaded balls are Na^+ cations. The notation $U(m, n)$ specifies the distortion ΔU_n experienced by the ions in the mth coordination shell (see table 1 for quantitative values).

a KCl host lattice [38]. Due to the different host materials considered, it is not possible to make a quantitative comparison between the two works. At a qualitative level, the main difference found in reference [38] between the KCl distortions around D_{4h} and D_{2h} defect configurations is that the Tl^+–Tl^+ distance expands in the first case and contracts in the second case, compared to the K^+–K^+ distance. The contraction of the Tl^+–Tl^+ distance in the D_{2h} centre is explained by the fact that expansion of the two anions at $(U_2, -U_2, 0)$ allows the Tl^+ cations to approach each other by reducing the electron cloud repulsion. In the iodides considered in this work, we always obtain an expansion of the Tl^+–Tl^+ distance, irrespective of the defect configuration. Nevertheless, using the same argument as was advanced by Pascual *et al* we expect the approach of the two Tl^+ cations along the (110) direction to be substantially impeded in NaI and KI as compared to KCl, simply because of the much larger size of iodide anions compared to chloride anions. Moreover, we obtain a smaller Tl^+–Tl^+ equilibrium distance in NaI as compared to KI, correlating with a larger expansion of the two anions at $(U_2, -U_2, 0)$. Thus, the qualitative trends seem to agree with those found by Pascual *et al* [38].

3.2. Relative stabilities of D_{4h} and D_{2h} defect configurations

To analyse the relative stability of the two different defect configurations at conditions of low pressure and temperature, we calculate their respective formation energies, given in terms of the internal energy difference for the following solid-state exchange reaction:

$$(A^+{:}AX)_s + 2Tl^+_g \rightleftharpoons ((Tl^+)_2{:}AX)_s + 2A^+_g \tag{8}$$

where the subscripts s and g refer to solid and gas phases, respectively. In order to take into account possible (electronic) lattice polarization effects, we have enlarged the active clusters with a PIM description of additional ions fixed at their lattice positions. An active cluster of

1000 ions, centred in the defect region, has been considered. For this cluster size, the induced dipoles on the more distant ions are already negligibly small, so lattice polarization effects do not extend beyond this relatively small region for the isovalent defects that we are considering. We show in table 3 the different contributions to the formation energies of the defects and to their relative stabilities. A negative energy contribution acts to stabilize the defect, while a positive energy contribution tends to destabilize it. As the Madelung energy is minimized (for a given lattice parameter) by the perfect crystal geometry, the Coulomb energy always tends to destabilize the defects. The larger the lattice distortion induced by the impurity, the larger this energy contribution. Correspondingly, it is always larger for the NaI host lattice, as compared to KI. For both host lattices, we can also see that the distortion is greater in the D_{4h} than in the D_{2h} configuration. Significant differences are seen in the contribution of short-range repulsion interactions to the formation energies of the Tl^+-dimer defect. While in KI this contribution tends to stabilize the defect, the opposite holds for NaI. The reason for this is that the mismatch effect is much more important in NaI, and the calculated lattice relaxation around the defect is not efficient enough in reducing the overlap repulsions. In KI, in contrast, the mismatch effect is much smaller and lattice relaxation induces a decrease in the overlap repulsions which is enough to stabilize the defect. For both crystals, the repulsive contribution to the relative stability of the two defect configurations opposes that of the Coulomb interaction. The inclusion of dispersion and polarization interactions in the calculation of the formation energy is therefore crucial in the case of NaI, as the defect would be predicted to be unstable at 0 K if one omitted these terms. Concerning the relative stability of the two configurations, both dispersion and polarization interactions tend to stabilize the D_{4h} defect, by small but significant amounts, given the large cancellation found between Coulombic and short-range repulsive interactions. In the case of the (short-ranged) dispersion interactions, this is easily rationalized: the bonds contributing the most to the dispersion are the Tl^+–I^- bonds, and in the D_{4h} defect one more Tl^+–I^- bond is formed in comparison with the D_{2h} defect. The polarization contribution to the energy of the pure crystals is strictly zero, so its contribution to the formation energy of the defects is highly relevant, and can be considered another (more indirect) measure of lattice distortion. On adding all the different energy contributions, the D_{4h} configuration is lower in energy for both crystals. However, in the case of NaI, those two configurations are so close in energy that they should be considered instead as degenerate for all practical purposes.

Table 3. Different contributions to the formation energies and to the relative stabilities of D_{4h} and D_{2h} configurations of the Tl^+-dimer impurity in NaI and KI. The relative stabilities are quoted, so a negative contribution implies a higher stability for the D_{4h} configuration. All quantities are in eV.

NaI	D_{4h}	D_{2h}	Difference	KI	D_{4h}	D_{2h}	Difference
Coulomb	0.57	0.49	0.08	Coulomb	0.44	0.42	0.02
Sr repulsion	2.78	2.88	−0.10	Sr repulsion	−0.62	−0.42	−0.020
Dispersion	−2.40	−2.38	−0.02	Dispersion	−1.04	−1.02	−0.02
Polarization	−1.57	−1.54	−0.03	Polarization	−0.95	−0.94	−0.01
Total	−0.62	−0.55	−0.07	Total	−2.37	−1.96	−0.21

4. Conclusions

In this paper it has been stressed that computer simulations of lattice distortions induced by substitutional impurities are likely to be significantly affected by the size of the active cluster

employed to simulate those distortions. Specifically, it has been found that at least first- and second-coordination-shell distortions around the defect have to be considered in order to obtain reliable results for the distortion around a Tl^+ dimer in alkali halides. To obtain full convergence for those distortions, one also has to allow for relaxation of at least third and fourth coordination shells. This is due to the strong coupling between the distortions experienced by different coordination shells.

The lattice distortions around both D_{4h} and D_{2h} defect configurations of a Tl^+-dimer impurity in NaI and KI host lattices have been described. The results conform with the expectation that these distortions should be greater in NaI as compared to KI, due to a larger size mismatch effect. The relative stability of the two different configurations at zero pressure and temperature conditions has been analysed in terms of Coulomb, repulsion, dispersion and polarization energy components. The inclusion of dispersion and polarization is mandatory in the case of NaI, as the consideration of only Coulomb and short-range repulsion effects predicts the defect to be unstable. Although the theoretical predictions point towards a higher stability of the D_{4h} configuration in NaI, the energy difference is small enough for one to anticipate that the two configurations can coexist under normal experimental conditions. In the case of KI, however, the D_{4h} configuration is energetically favoured by 0.21 eV. An interesting question that deserves further attention is that of how entropic terms can affect the free-energy relative stabilities at finite temperatures.

Acknowledgments

The author is grateful to Angel Martín Pendás for providing him with the FORTRAN code VCALC, which was very helpful in the parametrization of the distortions. He also acknowledges the Ministerio de Educación y Ciencia for the award of a postdoctoral grant.

References

[1] Blasse G and Grabmaier B C 1995 *Luminescent Materials* (Berlin: Springer)
[2] Barkyoumb J H and Mansour A N 1992 *Phys. Rev.* B **46** 8768
[3] Pong W F, Mayanovic R A, Bunker B A, Furdyna J K and Debska U 1990 *Phys. Rev.* B **41** 8440
[4] Zaldo C, Prieto C, Dexpert H and Fessler P 1991 *J. Phys.: Condens. Matter* **3** 4135
[5] Aramburu J A, Moreno M, Cabria I, Barriuso M T, Sousa C, de Graaf C and Illás F 2000 *Phys. Rev.* B **62** 13 356
Sousa C, de Graaf C, Illás F, Barriuso M T, Aramburu J A and Moreno M 2000 *Phys. Rev.* B **62** 13 366
[6] Aguado A, Ayuela A, López J M and Alonso J A 1998 *Phys. Rev.* B **58** 11 964
[7] Aguado A, López J M and Alonso J A 2000 *Phys. Rev.* B **62** 3086
[8] Aguado A 2000 *J. Chem. Phys.* **113** 8680
[9] Aguado A 2001 *J. Chem. Phys.* **114** 5256
[10] Aguado A 2001 *Physica B* submitted
[11] Tsuboi T and Jacobs P W M 1991 *J. Phys. Chem. Solids* **52** 69
[12] Yuster P H and Delbecq C H 1953 *J. Chem. Phys.* **21** 892
[13] Uchida Y and Kato R 1959 *J. Phys. Soc. Japan* **14** 1408
[14] Van Sciver W J 1960 *Phys. Rev.* **120** 1193
[15] Delbecq J H, Ghosh A K and Yuster P H 1966 *Phys. Rev.* **151** 599
[16] Matsui E 1967 *J. Phys. Soc. Japan* **22** 819
[17] Kaufman R G and Hadley W B 1967 *J. Chem. Phys.* **46** 1598
[18] Fontana M P and Van Sciver W J 1968 *Phys. Rev.* **168** 960
[19] Uchida Y and Tsuboi T 1968 *J. Phys. Soc. Japan* **24** 1075
Uchida Y and Tsuboi T 1970 *J. Phys. Soc. Japan* **29** 1303
[20] Ranfagni A, Pazzi G P, Fabeni P, Vilani G and Fontana M P 1972 *Phys. Rev. Lett.* **28** 1035
[21] Yoshikawa A, Takezoe H, Murayama I and Onaka R 1972 *J. Phys. Soc. Japan* **32** 472
Yoshikawa A, Takezoe H and Onaka R 1972 *J. Phys. Soc. Japan* **33** 1632

[22] Ermoshkin A, Evarestov R, Gindina R, Maaroos A, Osminin V and Zazubovich S 1975 *Phys. Status Solidi* b **70** 749
[23] Yoshikawa A and Onaka R 1975 *J. Phys. Soc. Japan* **38** 804
Yoshikawa A and Onaka R 1975 *J. Phys. Soc. Japan* **38** 810
[24] Koshino S, Ohata T and Hayashi T 1980 *J. Phys. Soc. Japan* **49** 1387
[25] Joshi R V and Nene J G 1982 *Z. Phys.* B **46** 13
[26] Tsuboi T 1984 *Phys. Rev.* B **29** 1022
[27] Joosen W, Goovaerts E and Schoemaker D 1987 *Phys. Rev.* B **35** 8215
[28] Fleurent H, Schoemaker D and Joosen W 1990 *Phys. Rev.* B **41** 10 138
[29] Tsuboi T, Polosan S and Topa V 2000 *Phys. Status Solidi* b **217** 975
[30] Tsuboi T, Zota S and Topa V 2001 *Physica* B **293** 333
[31] Herb G K, Fontana M P and Van Sciver W J 1968 *Phys. Rev.* **168** 1000
[32] Zazubovich S 1970 *Opt. Spectrosc.* **28** 392
[33] Tsuboi T and Jacobs P W M 1975 *J. Lumin.* **11** 227
[34] Ohata T, Hayashi T and Koshino S 1980 *J. Phys. Soc. Japan* **48** 1193
[35] Tsuboi T 1980 *Phys. Status Solidi* b **102** K7
Tsuboi T 1981 *Phys. Status Solidi* b **106** 301
[36] Tsuboi T 1984 *Phys. Rev.* B **29** 4755
[37] Benci S and Fermi F 1985 *Phys. Rev.* B **32** 2554
Benci S, Chiari A and Fermi F 1986 *Phys. Rev.* B **34** 5769
[38] Pascual J L, Barandiarán Z and Seijo L 2001 *J. Molec. Struct. (Theochem)* **537** 151
[39] Luaña V and Pueyo L 1990 *Phys. Rev.* B **41** 3800
[40] Luaña V, Recio J M and Pueyo L 1990 *Phys. Rev.* B **42** 1791
[41] Pueyo L, Luaña V, Flórez M and Francisco E 1992 *Structure, Interactions and Reactivity* vol B, ed S Fraga (Amsterdam: Elsevier) p 504
[42] Luaña V, Flórez M, Francisco E, Martín Pendás A, Recio J M, Bermejo M and Pueyo L 1992 *Cluster Models for Surface and Bulk Phenomena* ed G Pacchioni, P S Bagus and F Parmigiani (New York: Plenum) p 605
[43] Luaña V, Martín Pendás A, Recio J M and Francisco E 1993 *Comput. Phys. Commun.* **77** 107
[44] Blanco M A, Martín Pendás A and Luaña V 1997 *Comput. Phys. Commun.* **103** 287
[45] Huzinaga S, Seijo L, Barandiarán Z and Klobukowski M 1987 *J. Chem. Phys.* **86** 2132
[46] Luaña V and Flórez M 1992 *J. Chem. Phys.* **97** 6544
[47] Luaña V, Flórez M and Pueyo L 1993 *J. Chem. Phys.* **99** 7970
[48] Flórez M, Blanco M A, Luaña V and Pueyo L 1994 *Phys. Rev.* B **49** 69
[49] Huzinaga S and Cantu A A 1971 *J. Chem. Phys.* **55** 5543
[50] Huzinaga S, McWilliams D and Cantu A A 1973 *Adv. Quantum Chem.* **7** 183
[51] McWeeny R 1989 *Methods of Molecular Quantum Mechanics* (London: Academic)
[52] Pyper N C 2001 *J. Chem. Phys.* **114** 4390
[53] Francisco E, Martín Pendás A and Adams W H 1992 *J. Chem. Phys.* **97** 6504
[54] Aguado A, Ayuela A, López J M and Alonso J A 1997 *J. Phys. Chem.* B **101** 5944
[55] Clementi E 1965 *IBM J. Res. Dev.* **9** 2
[56] Chakravorty S J and Clementi E 1989 *Phys. Rev.* A **39** 2290
[57] Clementi E 2000 *IBM J. Res. Dev.* **44** 228
[58] Wilson M, Madden P A, Pyper N C and Harding J H 1996 *J. Chem. Phys.* **104** 8068
[59] Rowley A, J̌emmer P, Wilson M and Madden P A 1998 *J. Chem. Phys.* **108** 10 209
[60] Marks N A, Finnis M W, Harding J H and Pyper N C 2001 *J. Chem. Phys.* **114** 4406
[61] Clementi E and Roetti C 1974 *At. Data Nucl. Data Tables* **14** 177
[62] McLean A D and McLean R S 1981 *At. Data Nucl. Data Tables* **26** 197
[63] Ashcroft N M and Mermin N D 1976 *Solid State Physics* (New York: Holt, Rinehart and Winston)
[64] Madden P A and Wilson M 1996 *Chem. Soc. Rev.* **25** 399
[65] J̌emmer P, Wilson M, Madden P A and Fowler P W 1999 *J. Chem. Phys.* **111** 2038
[66] Aguado A, López-Gejo F and López J M 1999 *J. Chem. Phys.* **110** 4788
[67] Aguado A and López J M 2000 *J. Phys. Chem.* B **104** 8398
[68] See, for example,
Hutchinson F, Wilson M and Madden P A 2000 *J. Phys.: Condens. Matter* **12** 10 389
Domene C, Fowler P W, Wilson M, Madden P A and Wheatley R J 2001 *Chem. Phys. Lett.* **333** 403
and references therein.
[69] Fowler P W and Pyper N C 1985 *Proc. R. Soc.* A **398** 377
[70] Pyper N C 1986 *Phil. Trans. R. Soc.* A **320** 107

[71] Pyper N C 1991 *Adv. Solid State Chem.* **2** 223
[72] Slater J C and Kirkwood J G 1931 *Phys. Rev.* **37** 682
[73] Al-Abdalla A, Seijo L and Barandiarán Z, unpublished results
[74] Barriuso M T, Aramburu J A and Moreno M 1999 *J. Phys.: Condens. Matter* **11** L525
[75] Martín Pendás A 1999 private communication
[76] Wyckoff R W G 1963 *Crystal Structures* vol 1 (New York: Interscience)
[77] Matsuoka O, Pisani L and Clementi E 1993 *Chem. Phys. Lett.* **202** 13
[78] Wang F, Hong G Y and Li L M 2001 *Chem. Phys.* **263** 271
[79] Barandiarán Z and Seijo L 1994 *J. Chem. Phys.* **101** 4049
[80] Metz B, Stoll H and Dolg M 2000 *J. Chem. Phys.* **113** 2563